



Get Clarity On Generics

Cost-Effective CT & MRI Contrast Agents



**FRESENIUS
KABI**

[WATCH VIDEO](#)

AJNR

Common and Expected Postmortem CT Observations Involving the Brain: Mimics of Antemortem Pathology

A.B. Smith, G.E. Lattin, Jr., P. Berran and H.T. Harcke

AJNR Am J Neuroradiol 2012, 33 (7) 1387-1391

doi: <https://doi.org/10.3174/ajnr.A2966>

<http://www.ajnr.org/content/33/7/1387>

This information is current as of August 18, 2025.

ORIGINAL RESEARCH

A.B. Smith
G.E. Lattin, Jr.
P. Berran
H.T. Harcke

Common and Expected Postmortem CT Observations Involving the Brain: Mimics of Antemortem Pathology

BACKGROUND AND PURPOSE: Postmortem imaging with CT or MR is emerging as an effective technique to augment forensic autopsy. Expected findings on postmortem imaging of the brain may mimic pathologic processes in the living brain, leading to potential misdiagnosis. The purpose of this study is to describe the array of CT findings that can be expected to be present within the brain after death.

MATERIALS AND METHODS: A retrospective review was performed using an anonymized data base of 33 postmortem head CTs with no evidence of trauma to the face or scalp. Head CTs were assessed for 1) loss of gray-white differentiation, 2) effacement of the ventricles and cisterns, 3) postmortem intravascular blood distribution, 4) presence of intracranial or intravascular air, and 5) an irregular appearance of the falx. Imaging findings were correlated with autopsy findings.

RESULTS: Visualization of the basal ganglia was noted in 30 (91%) subjects, and the cortical ribbon was appreciated in 14 (42%). The ventricles and cisterns were effaced in 19 (58%) cases. An "expected postmortem blood distribution" was seen in 27 (82%) instances. Intravascular air was present in 14 cases (42%). A "lumpy" falx was present in 20 cases (61%). In 4 cases of subdural or subarachnoid hemorrhage noted on autopsy, but not on CT, retrospective review confirmed that a true discrepancy between the radiology and pathology findings persisted.

CONCLUSIONS: Recognition of expected postmortem patterns is required before pathology can be accurately diagnosed. A limitation of CT virtual autopsy is the possibility of missing small blood collections.

ABBREVIATION: MDCT = multidetector CT

It has been demonstrated that postmortem MDCT, or virtual autopsy, is complementary to forensic autopsy.¹⁻³ As virtual autopsy gains more widespread utilization, an understanding of the imaging findings that reflect the normal decomposition process is essential to prevent misinterpretation of normal postmortem radiologic findings as pathologic processes. The goal of this article is to characterize the expected imaging findings in the postmortem brain in the 72 hours after death and to describe the pitfalls in imaging interpretation that could lead to an incorrect diagnosis.

Materials and Methods

Patients

A retrospective review was performed using an anonymized data base of 33 postmortem head CT scans from autopsied cases with no evidence of trauma to the face or scalp and an intact calvaria. The 33 cases were divided as to cause of death, with 24 cases associated with trau-

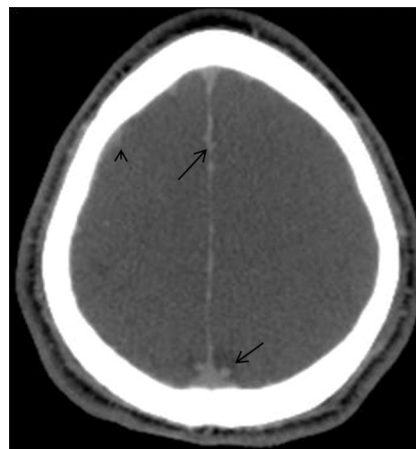


Fig 1. The "lumpy" falx. Axial noncontrast CT image demonstrates irregularity along the falx (arrows). This is related to high attenuation within the venous structures and not subarachnoid hemorrhage. More peripherally located venous structures also demonstrate high attenuation (arrowhead).

matic (penetrating) injury to areas other than the head or brain and 9 cases associated with nontraumatic causes not related to intracranial pathology (cardiac-related pathology). Imaging findings were cataloged and correlated with intracranial autopsy findings. The time from death to imaging was within 72 hours. Subjects had been maintained in a cooled environment as soon after death as possible, but times varied. However, all were in the early stages of decomposition, as judged by absence of settling or liquefaction of the brain. Data on sex and age were not available, other than all subjects were between 18 and 65 years of age.

Received September 14, 2011; accepted after revision November 9.

From the Armed Forces Institute of Pathology, Department of Radiologic Pathology (A.B.S., G.E.L., H.T.H.), Washington, DC; Uniformed Services University of the Health Sciences (A.B.S., G.E.L., H.T.H.), Bethesda, Maryland; Armed Forces Medical Examiner System (P.B.), Rockville, Maryland.

Paper previously presented as an educational exhibit at: Annual Meeting of the Radiologic Society of North America, November 28–December 3, 2010; Chicago, Illinois.

The views herein are those of the authors and not of the US Department of Defense, US Army, or US Air Force.

Please address correspondence to Alice B. Smith, MD, Department of Radiology and Radiological Sciences, Uniformed Services University, 4301 Jones Bridge Rd, Bethesda, MD 20814; e-mail: alsmith@usuh.mil

<http://dx.doi.org/10.3174/ajnr.A2966>

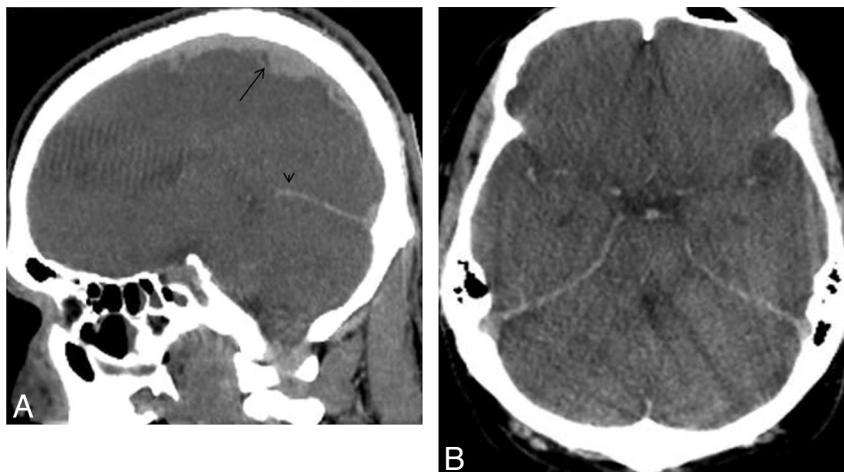


Fig 2. Increased vascular attenuation. *A*, Sagittal reformation from a noncontrast CT reveals high attenuation within the sagittal (arrow) and straight sinuses (arrowhead). The irregular appearance of the sagittal sinus is related to the cortical veins draining into the sinus. *B*, Axial noncontrast CT through the level of the circle of Willis reveals increased attenuation within the arteries. The beam-hardening artifact is related to the grommets on the human remains pouch.

Imaging Protocol

All imaging was performed on a LightSpeed 16 Xtra (GE Healthcare, Milwaukee, Wisconsin). The subjects remained in human remains pouches for the imaging. Whole body (head to toe) images were acquired helically in the axial plane, with a section thickness of 1.2 mm and a section interval of 1.3 mm, enabling reformations (mA 480 KV 120). In addition, axial 2.5-mm-section-thickness images of the head were also obtained with the CT gantry angled parallel to the orbital-meatal line. Imaging immediately preceded autopsy in all cases. A board-certified forensic pathologist performed the autopsies.

Imaging Review

The images were evaluated by a board-certified neuroradiologist with forensic radiology experience, a forensic radiologist with more than 10 years' experience in the field of forensic radiology, and a board-certified general radiologist with experience in forensic radiology. The evolving field of forensic radiology requires assessing imaging findings in a way that differs from assessing images from a living patient, so collaboration among radiologists with different areas of expertise was important. For their initial interpretation, the radiologists were blinded to the autopsy results. Evaluation of the imaging was performed using an Advantage workstation (software version 4.2_07; GE Healthcare). The imaging findings were then correlated

with autopsy findings to confirm that the observation was not the result of a pathologic process.

The focus of the image review was to document brain findings that would be pathologic in a living patient but that would become an expected observation after death as decomposition ensues. Five criteria were selected. Brain CT scans were assessed for 1) loss of gray-white differentiation, 2) effacement of the ventricles and cisterns, 3) blood distribution pattern, 4) presence of intracranial or intravascular air, and 5) an irregular or "lumpy" appearance of the falx (Fig 1). The radiologists applied the same criteria used in assessing the living brain, and images were manipulated for optimal window and level. Gray-white differentiation was judged by whether the basal ganglia or cortical ribbon was visible. Visualization of the gray-white differentiation was enhanced using narrow window and level (stroke window) ranges 21–56 W and 30–41 L. A recurring blood distribution pattern in the postmortem brain was recognized and termed "normal." It was described as increased attenuation involving the circle of Willis and dural venous sinuses (Fig 2). For intravascular air and irregular falx cases, presence versus absence was noted, with no attempt made at quantification.

Results

Visualization of the basal ganglia was noted in 30 (91%) cases (Fig 3), and the cortical ribbon was appreciated in 14 (42%). The ventricles and cisterns were effaced in 19 (58%) subjects. Normal postmortem blood distribution was seen in 27 (82%) instances. Intravascular air was present in the brain in 14 cases (42%). A lumpy falx was present in 20 cases (61%). The findings are summarized in the Table.

In 6 cases, differences between the radiologic and pathologic findings were present. After review of the autopsy findings and careful correlation with the images, there was consensus agreement that subarachnoid hemorrhage was recognized on the MDCT in 2 of these 6 cases. Thus, the images and autopsy were in agreement. In 4 cases, retrospective review confirmed that a true discrepancy between the radiology and pathology findings persisted in regard to detection of blood on the brain surface. In these cases where discrepancy persisted, it was concluded that MDCT did not demonstrate abnormality, despite knowledge of the location of the hemorrhage (sub-

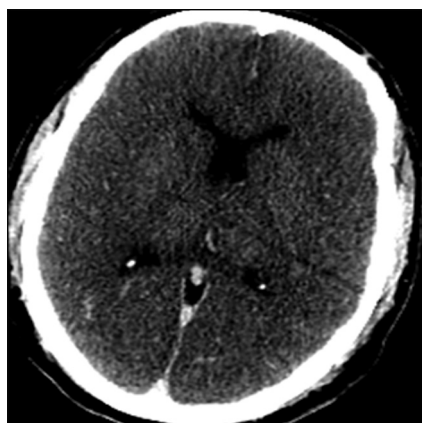


Fig 3. Visualization of the basal ganglia. Axial CT using narrow window and level (50W 35 L) allows for visualization of both the basal ganglia and thalami.

Postmortem Imaging Findings					
Case Type	Loss of G–W Differentiation	Effaced Ventricles/Cisterns	Expected PM Blood Distribution	PM Intracranial Air	Lumpy Falx
Trauma	Visible BG 22/24 Loss of G–W 7/24	Yes 15/24 Normal 8/24 Dilated 1/24	Yes 19/24 SAH 4/24	12/24	12/24
Natural cause of death	Visible BG 8/9 Loss of G–W 7/9	Yes 4/9 Normal 5/9	Yes 8/9	2/9	8/9

Note:—Loss of G–W differentiation evaluated by whether BG visible and whether remaining G–W visible. Expected PM blood distribution = dense circle of Willis, cavernous sinus, tentorium, transverse sinus, sagittal sinus. PM Intracranial Air = air in the arteries, veins, or diploic spaces. Lumpy Falx = nodular appearance to falx seen in PM imaging. BG indicates basal ganglia; G–W, gray–white; PM, postmortem.

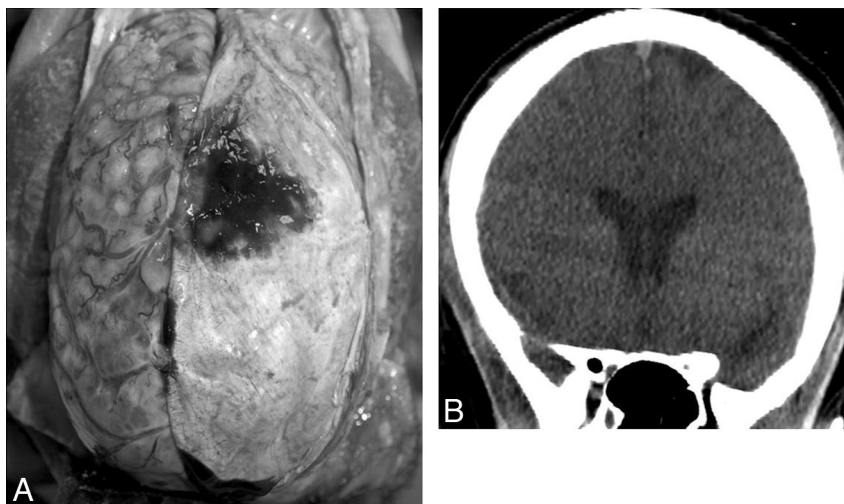


Fig 4. Bilateral subdural hemorrhage not seen on CT. *A*, Photograph from autopsy in which the left aspect of the dura has been reflected to the right, revealing the left-sided subdural hematoma that is adherent to the dura. Note that viewing the brain from above changes right–left orientation from the convention used on CT. *B*, Noncontrast CT coronal reformat from the same subject does not demonstrate subdural hemorrhage. No evidence of hemorrhage was seen on the original axial images or the sagittal reformation.

arachnoid in 3 cases, and bilateral subdural hematomas in 1) (Fig 4).

Discussion

Correlation of postmortem images and autopsy has significant medicolegal implications. One concern is that settling of blood in the venous sinuses and cortical veins can be confused with subarachnoid or subdural hemorrhage. Pathologists recog-

nize that normal postmortem decomposition never leads to subarachnoid or subdural hemorrhage. Our findings indicate that small collections can be both overlooked and undetectable with CT imaging, even when using reformations, which has been shown to improve detection in living patients.⁴ It has been previously demonstrated that a limitation of CT virtual autopsy is the possibility of missing very small collections of blood. Yen et al⁵ evaluated postmortem brains with traumatic injury and found that CT had a sensitivity of 73% for the detection of subdural hemorrhage. In their study, the cases where the subdural hemorrhage was missed occurred when the blood layer in the forensic autopsy was less than 3 mm in thickness.⁵ This correlated with what was found in our study, and the etiology of the subarachnoid and subdural hemorrhage was presumed to be related to trauma, even though there was no obvious external or calvarial evidence of traumatic head injury. In these cases, the subjects had evidence of penetrating injury to other body regions. There was no evidence that subdural or subarachnoid hemorrhage was related to decomposition.

Other imaging findings depend on the rate of decomposition, which is variable, depending on factors including ambient temperature, body weight and size, and humidity.⁶ Cerebral autolysis is present, to some degree, in bodies autopsied after 24 hours. Imaging findings of this phenomenon include blurring or loss of the gray–white junction, decrease in cerebral attenuation, and effacement of the sulci and ventricles (Fig 5).⁶ Our visualization of cortical ribbon in 42% and basal



Fig 5. Cerebral autolysis. Noncontrast CT reveals low cerebral attenuation, with loss of the gray–white differentiation, and sulcal and cisternal effacement.

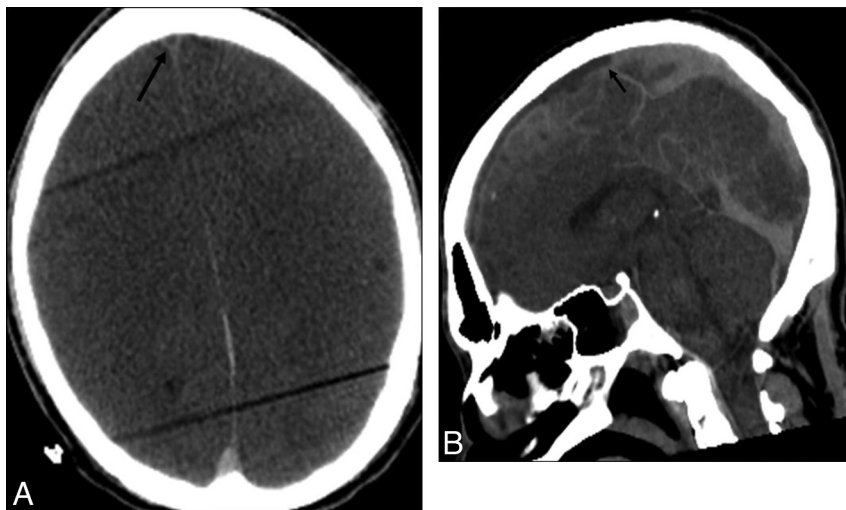


Fig 6. Hematocrit effect. *A*, Axial noncontrast CT reveals high attenuation within the posterior aspect of the sagittal sinus but low attenuation within the anterior aspect of the sinus (arrow). Beam-hardening artifact is caused by the grommets on the body bag. *B*, Sagittal reformation demonstrates the fluid–fluid level in the sagittal sinus (arrow).

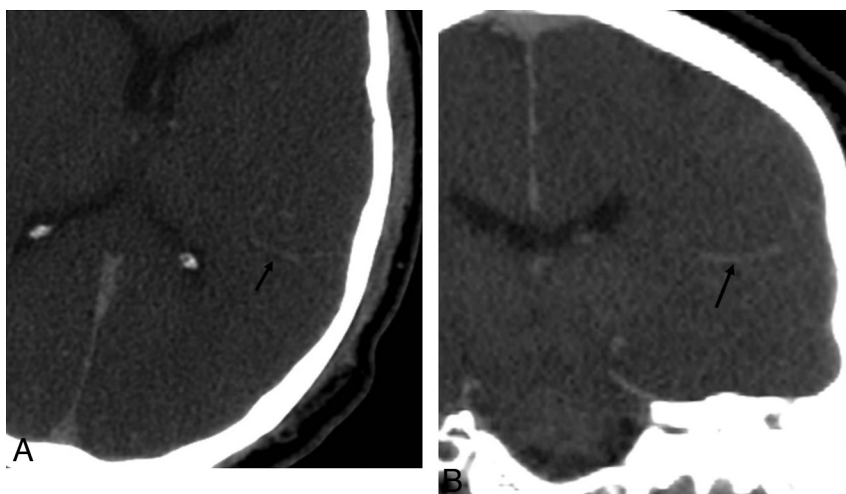


Fig 7. Hyperattenuating vein. Axial (*A*) and coronal reformat (*B*) noncontrast CT demonstrates a hyperattenuating vein in the left tempoparietal region (arrows). This should not be mistaken for subarachnoid hemorrhage.

ganglia in 91% confirm the need for proper windowing to see the deep gray matter.

The “expected postmortem blood distribution” is attributed to postmortem hypostasis. Livor mortis, or postmortem hypostasis, results in increased attenuation within the dependent aspects of blood vessels. A hematocrit effect with fluid levels may be seen in the larger vessels (Fig 6). This results from the higher attenuation erythrocytes layering in the dependent portion of the vessel. One study reported that this phenomenon may be seen on imaging within 2 hours after death.⁷ In a body that has remained in the supine position since death, high attenuation may be seen in the posterior sagittal sinus, straight sinus, and transverse sinuses.⁶

Increased arterial attenuation is secondary to hemoconcentration, and this finding should not be mistaken for subarachnoid hemorrhage. The venous structures will also demonstrate increased attenuation due to hemoconcentration, and this should not be mistaken for dural sinus thrombosis unless there are additional findings to suggest acute thrombosis, such as venous infarction.⁶ Frequently, a prominent hy-

perattenuating vein was noted in the temporo-parietal region (Fig 7). This may be unilateral and should not be confused with subarachnoid hemorrhage.

Putrefactive gas may be seen, to variable degrees, within the arterial and venous structures, and it is typically symmetrically distributed (Fig 8)⁶; however, positioning of the head to one side or the other may result in more air on the nondependent side. It should not be mistaken for a pathologic gas collection, such as an air embolus, and is frequently missed on forensic autopsy.⁵ It should be noted that finding air in the postmortem brain is directly related to air in the vascular system in general, so variability is linked to decomposition in the torso. We do not believe vascular air in the brain is an isolated occurrence.

The lumpy falx appearance is secondary to the hyperattenuating cortical veins abutting the falx. Understanding that these vessels may be misinterpreted as subarachnoid hemorrhage is important. In a study by Yen et al,⁵ close to 20% of cases were falsely diagnosed with subarachnoid hemorrhage on postmortem imaging.

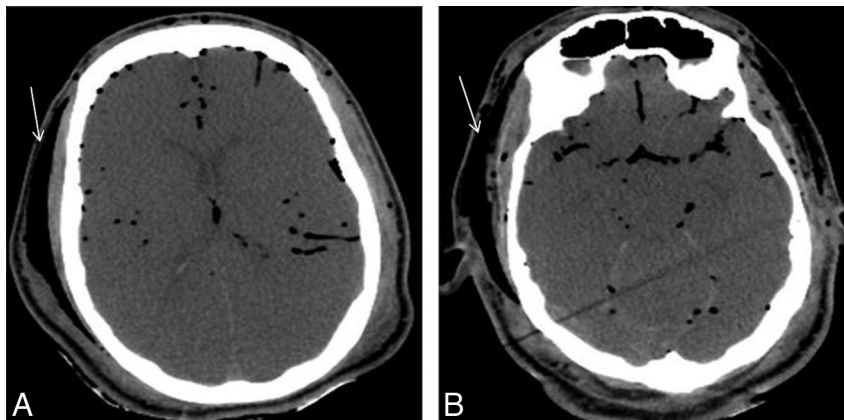


Fig 8. Vascular air. Axial noncontrast CT images demonstrate air within both the arterial and venous structures, which is relatively symmetrically distributed. In addition, air is seen within the subcutaneous tissues (arrows).

Major limitations of this study relate to the absence of specific timing from death to autopsy and the nature of preservation. Consequently, we are not able to determine the order in which brain changes occur and how they may interrelate. It would be very helpful to know whether postmortem brain findings might be linked to time of death, but this would require a carefully controlled study in which serial CT imaging is conducted on cases where time of death is known and environmental circumstances can be controlled.

Conclusions

The “gold standard” for postmortem forensic evaluation is the forensic autopsy, but virtual autopsy is proving to be a useful adjunct. A limitation of CT virtual autopsy is the possibility of missing very small collections of blood. The “normal” array of CT findings that are expected to be present in the brain after death are pathologic in the antemortem brain. For example, increased attenuation within the vasculature may be mistaken for hemorrhage or thrombosis. Recognition of postmortem

patterns caused by decomposition is required before pathology can be accurately diagnosed.

Disclosures: H. Theodore Harcke—*UNRELATED: Royalties: Elsevier, Comments: Royalty payment for textbook written in 2010 (title: *Essentials of Forensic Imaging*).*

References

1. Levy AD, Abbott RM, Mallak CT, et al. **Virtual autopsy: preliminary experience in high-velocity gunshot wound victims.** *Radiology* 2006;240:522–28
2. Thali MJ, Jackowski C, Oesterhelweg, et al. **VIRTopsy—the Swiss virtual autopsy approach.** *Leg Med (Tokyo)* 2007;9:100–04
3. Thali MJ, Yen K, Schweitzer, et al. **Virtopsy, a new imaging horizon in forensic pathology: virtual autopsy by postmortem multislice computed tomography (MSCT) and magnetic resonance imaging (MRI)—a feasibility study.** *J Forensic Sci* 2003;48:386–403
4. Wei SC, Ulmer S, Lev MH, et al. **Value of coronal reformations in the CT evaluation of acute head trauma.** *AJNR Am J Neuroradiol* 2010;31:334–39
5. Yen K, Lovblad K-O, Scheurer E, et al. **Post-mortem forensic neuroimaging: correlation of MSCT and MRI findings with autopsy results.** *Forensic Sci Int* 2007;173:21–35
6. Levy AD, Harcke HT, Mallak CT. **Postmortem imaging: MDCT features of postmortem change and decomposition.** *Am J Forensic Med Pathol* 31:12–17
7. Shiotani S, Kohno M, Ohashi N, et al. **Postmortem intravascular high-density fluid level (hypostasis): CT findings.** *J Comput Assist Tomogr* 2002;26:892–93